Available online at www.sciencedirect.com
ScienceDirect
Thermochimica Acta 461 (2007) 145–152
thermochimica acta
www.elsevier.com/locate/tca

An analysis of the meta stable structure of poly(ethylene terephthalate) by conventional DSC

Jürgen E.K. Schawe

Mettler-Toledo AG, Sonnenbergstrasse 74, CH-8603 Schwerzenbach, Switzerland

Available online 31 May 2007

Abstract

Semicrystalline polymers have a metastable structure. During heating, reorganization processes can occur at temperatures between the glass transition and the final melting. When DSC measurements are performed at conventional heating rates, reorientation can occur. This can be the reason why the measured melting peaks are not representative of the crystalline structure of the original material. At fast heating rates, the actual heating time is so short that practical no reorientation occurs during the measurement. A commercially available heat flux DSC (METTLER TOLEDO DSC822^e) was used to investigate the influence of heating rate on reorientation at heating rates between 1 K/min and 400 K/min. The measurements were performed on amorphous and semicrystalline poly(ethylene terephthalate), PET.

The heating rate dependence of the apparent glass transition temperature is discussed. For amorphous material, a criterion is given to estimate the minimum heating rate at which reorientation no longer occurs. Direct measurement of the melting of the crystallites present in the original starting material was possible at heating rates above 300 K/min. The original degree of crystallinity was approximately 1%. In the case of semicrystalline PET, the minimum heating rate at which recrystallization processes become less important, was determined using an Illers plot.

Keywords: Glass transition; Melting; Semicrystalline polymer

1. Introduction

The actual morphology of a polymeric material is influenced by its molecular structure and non-molecular factors such as its thermal and mechanical history, nucleating agents, and processing conditions. The morphology is usually characterized by crystallites. These are arranged in lamellas of different thickness, with rigid amorphous material on the surface of the lamellas and mobile amorphous phases between the crystallites [1]. This complex structure is metastable. Below the glass transition temperature, the structure of a semicrystalline polymeric material is almost completely stable due to the very slow molecular dynamics in the vitrified material. Above the glass transition temperature, the mobile amorphous component becomes liquid and small crystallites may melt at relative low temperatures. Consequently, reorganization can occur depending on the temperature and time regime [2]. Because of its moderate crystallization rate, poly(ethylene terephthalate) (PET) is often used as a model substance to study the reorientation processes. Reflecting the actual discussion about the metastable structure of polymers and of the reorganization phenomena it is interesting to recapitulate that this topic was up-to date in the 60th of the 20-century [3] and is it still [4,5].

Conventional DSC is usually performed at heating rates of up to 20 K/min. Due to the metastable morphology of polymeric materials, the resulting curves are however influenced by melting and recrystallization processes occurring during the measurement. In other words, the curves include information about the sample material relating to its thermal history and to the actual measurement conditions. The thermal effects of reorientation mask the thermal behavior due to the melting of the crystallits of the original material, i.e. the material as it was initially before the beginning of the first measurement. The use of fast DSC heating rates has been proposed by Mathot et al. [4,5] to prevent or minimize the influence of reorientation during measurement. These DSC applications were performed at heating rates of several 100 K/min. Such fast heating rates also improve sample throughput, and allow sample weights in the sub-milligram range to be measured. Schick et al. have shown in Refs. [6,7] that the heating rates can be expand above 10,000 K/min using dedicated chip calorimeter. To reduce the thermal lag in this method samples with a typical mass of 400 ng were placed directly on the sensor. By this new technique the advantage of the high heating rates

E-mail address: Juergen.Schawe@mt.com.

0040-6031/$ – see front matter © 2007 Elsevier B.V. All rights reserved.
doi:10.1016/j.tca.2007.05.017

is connected with problems at the sample mass determination. Practically the samples cannot be removed from the sensor.

In this paper we show for the example of PET that also the widely used conventional heat flux calorimeter can delivers fundamental information about the reorganization of semicrystalline polymers up to heating rates of 400 K/min and present simple rules for data evaluation and interpretation.

2. Experimental

The DSC measurements were performed with a METTLER TOLEDO DSC822^e equipped with the FRS5 DSC sensor, intracooler and sample robot. Nitrogen at 20 ml/min was used as purge gas. The samples measured in commercially available 20 μl aluminum crucibles with lids.

Small errors in calibration that do not significantly influence the accuracy of conventional measurements could give rise to appreciably larger deviations at faster heating rates. The DSC was therefore carefully calibrated at higher heating rates, and particular attention was paid to the calibration of thermal lag, τ_{lag}.

Before calibration, τ_{lag} was set to zero. The instrument was calibrated using indium and zinc standards at heating rates between 5 K/min and 300 K/min. Peak onset temperatures were evaluated. Because of the thermal resistance between sample and sensor, the measured onset temperature increases linearly with increasing heating rate. In Fig. 1 the difference between the onset temperature, T_{on}, and the temperature of fusion, T_{fus}, is plotted against the heating rate, β. As expected, the measured data fits a linear equation in the heating rate range used:

$$T_{on} = T_{fus} + \Delta T + \frac{dT}{d\beta}\beta \quad (1)$$

where ΔT is the difference between the extrapolated onset temperature at heating rate zero, $T_{on}(0)$, and T_{fus} is the temperature of fusion. The thermal lag, $\tau_{lag} = dT/d\beta$, depends slightly on temperature. The values for Zn and In were determined to be $\tau_{lag}(417.6\,^\circ C) = 5.50$ s and $\tau_{lag}(156.6\,^\circ C) = 4.73$ s, respectively. The difference in the thermal lag is mainly given by the temperature dependence of the thermal conductivity of the sensor material. The $T_{on}(0)$ and τ_{lag} data of both calibration materials was used for the temperature calibration of the DSC according to standard calibration procedures [8]. For heat flow calibration, the enthalpies of fusion of both calibration materials were used. Special calibration procedures for fast and slow DSC measurements were not necessary because heat flow calibration is independent of the heating rate.

The validity of temperature and heat flow measurements performed at different heating rates with the calibrated experimental setup was checked using an indium standard. This material was available as a pellet of mass approximately 6 mg. The relatively large sample was used to analyse the behavior of the experimental setup for samples with heat capacities comparable to those of the polymer samples measured (mass approximately 1 mg, typical thickness 80 μm). To optimize thermal contact, the sample was pressed in the crucible and pre-melted. The samples were heated at rates of up to 400 K/min. The onset temperatures and peak areas of the measured melting peaks were evaluated. The results are shown in Fig. 2. The temperature deviations are of the order ±0.2 K. The scatter of the measured enthalpy of fusion is ±0.16%. This data shows that the experimental setup can be used for both slow and very fast heating rates.

3. Results and discussion

3.1. Amorphous PET

The freshly prepared PET samples (mass approximately 1 mg) were weighed into 20 μl Al crucibles with lids and placed in the sample robot for measurement in the DSC cell. The samples were rapidly cooled so that they all had the same thermal history. For cooling the sample was placed on a dray aluminum block, which was cooled by ice water. Immediately after this preparation process the samples were measured at heating rates between 10 K/min and 300 K/min by DSC. For comparison, the curves in Fig. 3 are normalized with respect to specific heat capacity units. Above the glass transition at around 80 °C, the sample exhibits cold-crystallization. Melting occurs around 240 °C. With increasing heating rate, the cold-crystallization

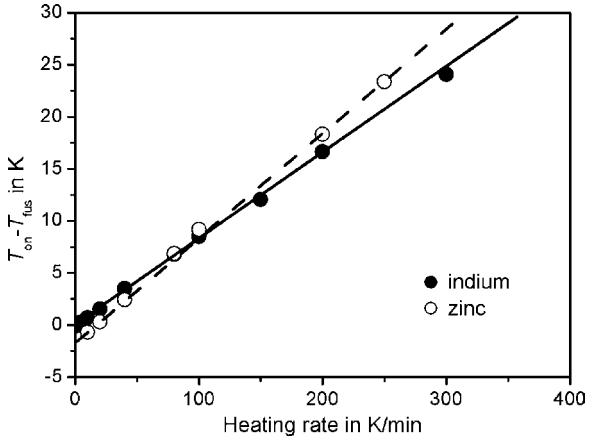

Fig. 1. The diagram displays the difference between the peak onset temperature and the temperature of fusion of the calibration material as a function of heating rate for an un-calibrated instrument.

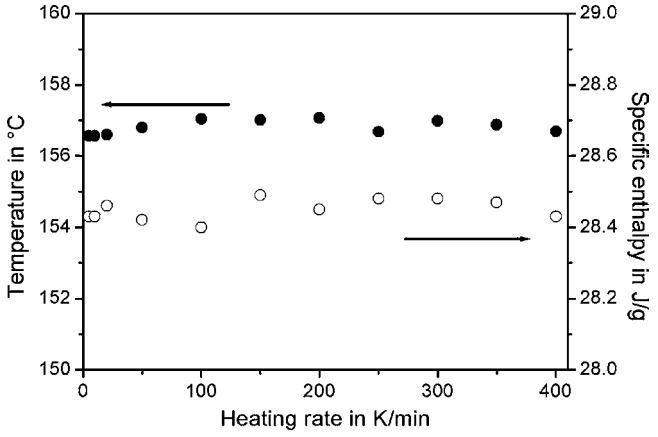

Fig. 2. Melting temperature (filled symbols) and enthalpy (open symbols) of indium measured at different heating rates after calibration.

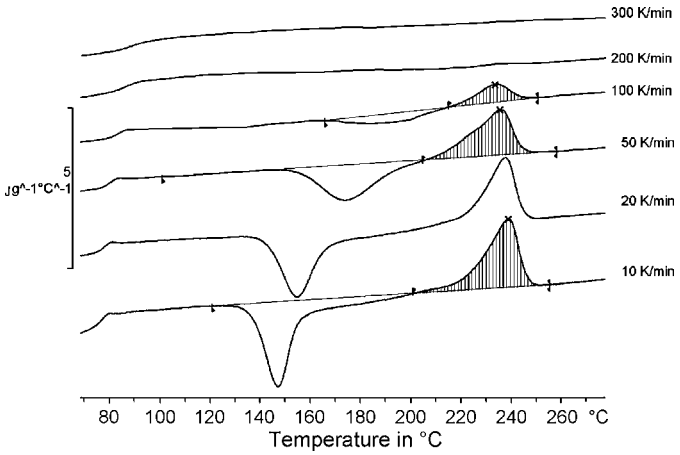

Fig. 3. DSC curves, in heat capacity units, of PET measured at different heating rates. The arrow indicates a small melting peak on the curve measured at 300 K/min. The evaluation of the melting peak area is shown on the example of the curves measured at 10, 50 and 100 K/min.

effect shifts to higher temperatures. The decreasing peak areas indicate that at faster heating rates the degree of crystallinity increases. The curves measured at slower heating rates do not characterize the original material because the main effects (crystallization and melting peaks) are induced by the measurement itself. At 200 K/min the melting peak and the induced processes are already very small. At 300 K/min, the absence of a melting peak around 240 °C indicates that no crystallization at all occurred during the measurement. This curve in fact characterizes the structure of the original material, because the recrystallization during heating at this high heating rate is suppressed. At first sight, only a glass transition is visible. In Ref. [4] a PET sample is measured at 100 K/min without significant indication of cold-crystallization. At this rate our material clearly shows reorganization. The reason for this different behavior is the faster crystallization of our material due to the added nucleating agent.

3.1.1. Heating rate dependence of the glass transition

In this section we concentrate on the glass transition and the melting behavior. The glass transition is often characterized by its temperature, T_g, and the step-height of the specific heat capacity, ΔC_p. The glass transition temperature is defined as the fictive temperature which characterizes the structure of the vitrified glass. It can be calculated by an enthalpic procedure described in Refs. [9–11]. Here we refer to T_g determined by such a procedure as the enthalpic glass transition temperature. The value of T_g depends on the cooling rate. During storage in the glassy state the enthalpic glass transition temperature decreases due to structural relaxation. If this relaxation practically does not occur during the time range between cooling and subsequent heating measurement the glass transition temperature should be dependent on the cooling rate. But it is independent on the heating rate [10–12]. The heating rate invariance of the enthalpic glass transition temperature is a consequence of the first law of thermodynamics (see Appendix A).

Thus the enthalpic glass transition temperature of annealed glasses depends only on the cooling rate. Any heating rate dependence must base on an additional effect which is related to the measuring technique. In the DSC the measured apparent enthalpic glass transition temperature is influence by smearing of the measured due to heat transfer in the measuring system (sensor, pan, sample, and thermal contacts). Smearing of the DSC curves shifts in a heating measurements the measured glass transition temperature to higher temperatures [13,14]. Thus the "apparent" glass transition temperature is higher than the actual glass transition temperature. The heating rate dependence of the apparent glass transition temperature can be described by the equation:

$$T_g(\beta) = T_{g0} + \beta\tau\left(1 - \exp\left(-\frac{T_{g0} - T_0}{\beta\tau} - 1\right)\right) \quad (2)$$

where T_{g0} is the glass transition temperature without smearing, T_0 a characteristic temperature that describes the onset of the glass transition and τ is a time constant, which is the characteristic time for the heat transfer between sample and sensor. The derivation of Eq. (2) is shown in Appendix B. For a slow heating rate, the exponent in Eq. (2) disappears and the glass transition temperature exhibits linear heating rate dependence. The fit of the data in Fig. 4 yields $T_{g0} = 76.2\,^\circ$C, $T_0 = 63.8\,^\circ$C, and $\tau = 3.18$ s. This data indicates that Eq. (2) is valid for heating rates below 470 K/min with the used experimental setup.

A comparison of T_{g0} with the glass transition temperatures published in Ref. [5] indicates that our data are about 5 K lower. This difference may be caused by chemical differences of the samples.

An alternative definition of the glass transition temperature is the temperature of the half step-height of the heat capacity change during the glass transition [15]. Because of the overheating effects during heating [10,11] such a glass transition temperature is normally higher than the apparent enthalpic glass transition temperature, and strongly depends on the actual curve shape. In the present case, the samples are rapidly cooled so that the heating rates are always smaller than the previous cooling rate. The curves show practically no enthalpy relaxation. The apparent enthalpic glass transition temperature is then practically equal to the half step-height temperature. The shift of the

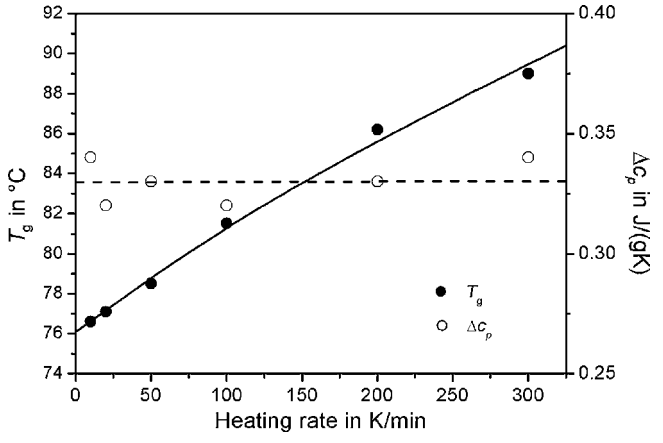

Fig. 4. Glass transition temperature, T_g, and step-height, ΔC_p, as a function of heating rate. The T_g values are fitted using Eq. (2).

glass transition temperature at different heating rates is determined mainly by the smearing of the signals between the sample and sensor.

Fig. 4 also displays the heat capacity change during glass transition, ΔC_p. As expected, there is no significant dependence of this value on the heating rate. This experimental result shows that heat capacity changes can be quantitatively determined at fast heating rates.

3.1.2. Melting peak analysis

The following discussion is based on the measured curves displayed in Fig. 3. At slow heating rates, the material remains in the liquid state above glass transition for a relatively long period of time. This time is long enough for the material to crystallize, melt and recrystallize during the measurement. The newly formed crystallites have a higher melting temperature than the original crystallites. Despite the change in morphology, the exothermic and endothermic heat contributions are equal if the degree of crystallinity does not change during this process. Consequently, the DSC curve shows a crystallization peak but does not show any evidence of recrystallization. On further heating, the crystallites undergo the recrystallization process many times, but the crystallization rate decreases because the sample temperature approaches the equilibrium melting temperature. As a result of this, the exothermic effects become smaller than the endothermic effects and the DSC curve shows a relative broad melting peak. At faster heating rates, the measured melting peak shifts to lower temperatures because less recrystallization. At 300 K/min, practically no melting in the relevant temperature range can be detected. The decrease of T_m with increasing heating rate is an indication of reorientation processes during measurement at slower heating rates.

During a DSC measurement melting occurs usually in a wide temperature range from temperatures short below the glass transition to the end of the melting peak. This is due to the distribution of the crystal size and the reorganization processes. For the evaluation of the enthalpy of such broad processes the selection of the right baseline is important. Especially in the case of semicrystalline polymers with a high original crystallinity the change of the baseline (or sensible) heat capacity becomes important due to reorganization and melting. This problem is detailed discussed in Refs. [16,17]. In the present case, the original material has after fast cooling a low crystallinity (it is almost amorphous). In this case a line given by the curve values before cold-crystallization and after the melting peak can be taken as the baseline for peak integration [18]. Both limits are determined by the heat capacity of the (almost) amorphous melt. The peak area of the melting peak (apparent enthalpy of fusion during melting) is evaluated using the described baseline. The temperature limits of integration are given be the intersection point between the baseline and the measured curve and a temperature above final melting (see. the curve measured at 50 K/min in Fig. 3).

As shown in Fig. 3, the area of the melting peak at 240 °C is influenced by the heating rate. Higher heating rates induce a lower degree crystallinity. A smaller apparent enthalpy of fusion, Δh_f, is therefore measured at higher heating rates. This dependence of Δh_f on β is shown in Fig. 5. On the basis of the observed behavior, we propose an exponential law to describe the relationship between Δh_f and β:

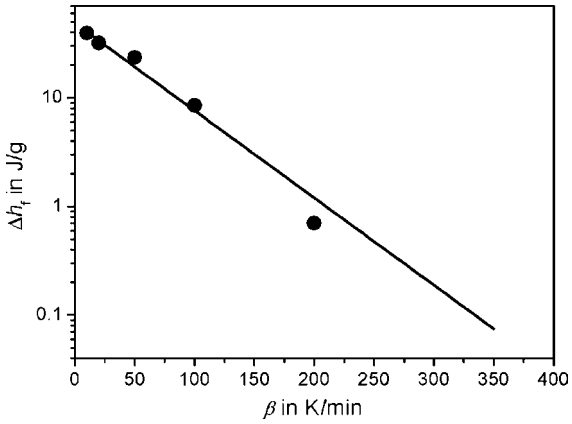

Fig. 5. Heating rate dependence of the enthalpy of fusion for the crystallites melting around 240 °C. The solid line is the fit result of Eq. (3).

$$\Delta h_f = \Delta h_f^\circ \exp\left(-\frac{\beta}{\beta_c}\right) \tag{3}$$

where Δh_f° is the specific enthalpy of fusion for infinitely slow heating and β_c is a characteristic heating rate. Using curve fitting, the parameters in Eq. (3) were determined to be $\Delta h_f^\circ = 48.5$ J/g and $\beta_c = 54$ K/min. The related curve is the solid line in Fig. 5.

The value of Δh_f° for fully crystallized material indicates a degree of crystallinity of 34.6%. (The equilibrium enthalpy of fusion Δh_f° of fully crystalline PET is taken to be 140 J/g [19].) An extrapolation of Eq. (3) to a heating rate of 300 K/min yields a value of approximately 0.2 J/g for the enthalpy of fusion of the crystallites formed during heating. Detailed examination of the curve in Fig. 3 does in fact show a very weak peak in the related temperature range 220–270 °C. We did not evaluate this peak because it seemed close to the limit of detection for the measurement.

According to Eq. (3), if the fade out parameter, β_c, is about five times larger than the actual heating rate, β, we can neglect crystallization during heating. This indicates that the minimum heating rate is 270 K/min at which recrystallization cannot be detected by the original amorphous material in the DSC curve. This agrees with the experimental results. Consequently, Eq. (3) can be used to estimate the minimum heating rate which avoids crystallization and reorganization.

3.2. Semicrystalline PET

In the case of isothermal crystallization, the size and stability of crystallites depends on the crystallization temperature. The lower the crystallization temperature, the less perfect the crystallites and the lower the expected melting temperature. However, imperfect crystallites are metastable. Such structures tend to recrystallize. Consequently, the melting temperature becomes heating rate dependent. Recrystallization increases the stability of the crystallites and shifts the peak temperature to higher temperatures. Nevertheless, it is usually of interest to measure the state of the semicrystalline polymer. To do this, the exper-

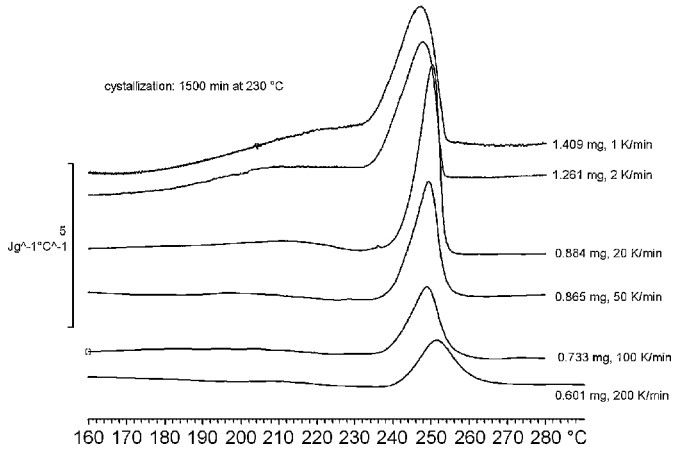

Fig. 6. DSC melting curves of PET crystallized at 230 °C for 1500 min in units of the specific heat capacity. The sample masses and heating rates used are given for each measurement.

imental conditions must be chosen so that no recrystallization occurs.

The PET samples were crystallized at a crystallization temperature, T_c, for a crystallization time, t_c in the preheated DSC cell. The samples were then rapidly cooled to room temperature and subsequently measured in the DSC at heating rates between 1 K/min and 350 K/min. Sample sizes were typically 2–0.5 mg. The samples were crystallized under three different sets of conditions: 200 °C for 50 min, 220 °C for 250 min, and 230 °C for 1500 min. Initial experiments have shown that the crystallization kinetics changes after sufficiently long storage of the sample in the melt. For this reason, new samples were used for each measurement.

Figs. 6 and 7 display the measured melting peaks for material that had been crystallized at 230 °C and 200 °C. The peak maximum temperature, T_m, is used to characterize the melting temperature. For the samples crystallized at 200 °C the melting peak shows a significant shoulder before its maximum at 2 K/min and 5 K/min. At 10 K/min the position of the maximum and the shoulder is exchanged. The melting of less stable crystals induces the lower temperature event. At the low rates the peak area increases with decreasing heating rate. This is

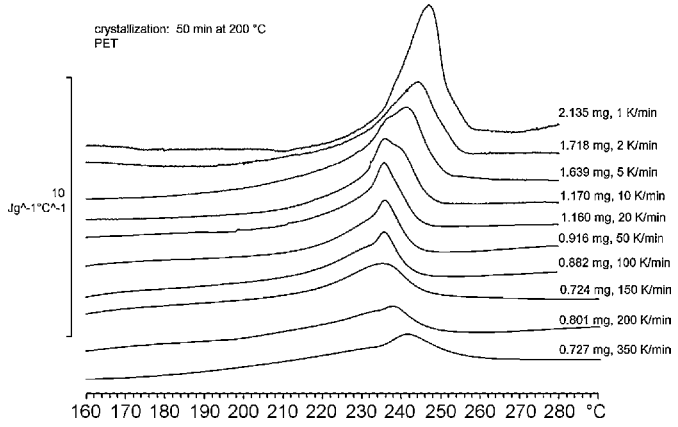

Fig. 7. DSC melting curves of PET crystallized at 200 °C for 50 min in units of the specific heat capacity.

an indication that also cold-crystallization occurs in addition to reorganization.

Fig. 7 shows that the peak maximum is at relatively high temperatures at the slowest heating rate. When the heating rate increases from 1 K/min to 20 K/min, T_m decreases. However, at heating rates above about 20 K/min, T_m increases at faster heating rates. Similar behavior is also observed when the samples are crystallized at the other temperatures. As has already been described above, the decrease of T_m with increasing heating rate at low values of β can be understood as a reorientation process of the metastable structure during heating. In contrast to such behavior, the peak maximum temperature increases at faster heating rates. This is due to heat transfer factors and is well known for the melting of pure metals such as indium. Furthermore, it is also a well-known effect that the peak maximum temperature increases if samples of larger mass are measured. This peak shift is caused by the thermal lag in the measuring cell due to heat transfer. The influence of reorientation and thermal lag on the melting curve of polymers was studied in detail by Illers some 30 years ago [20]. He found that the peak maximum temperature follows a square-root-law:

$$T_m = T_{m0} + A\sqrt{m\beta} \tag{4}$$

where T_m is the true melting temperature of the crystallites, m the sample mass, and A is a constant dependent on the actual specific enthalpy of fusion, Δh_f, and the thermal resistance, R, between the sample and sensor ($A = \sqrt{2R\Delta h_f}$). In the case of polymer melting we cannot neglect the heat transfer path inside the sample, due to its low heat conductivity. Thus R still plays a role, even in the case of thermal lag correction. This was shown by Wang and Harrison [21,22].

Illers proposed a method to determine the true melting temperature of polymer crystallites. This involved measurement of the melting behavior at different sufficiently fast heating rates followed by extrapolation to a heating rate of zero according to Eq. (4). As discussed below, the simple Illers approach delivers additional information about the recrystallization and melting behavior, even if in reality semicrystalline polymers are more complex. Especially one cannot distinguish between effects due to heat transfer and super heating of the crystals.

In Fig. 8, the maximum temperatures T_m for all the crystallization conditions used are plotted in the Illers plot. The peak maximum is indicated by a solid symbol and the shoulder by an open symbol. The melting behavior of the material crystallized at 230 °C follows an almost straight line in the measured heating rate range. The crystallites, which melt in the peak region, are relatively stable and practically no reorientation occurs during the DSC measurements. For $T_c = 220$ °C, the material exhibits reorientation during the measurement at heating rates of less than 20 K/min. Afterward, T_m also shows linear behavior in the Illers plot. In the main melting region reorganization becomes less importance. The crystallites produced by isothermal crystallization at 200 °C are less stable. At conventional heating rates, the melting of the original crystals cannot be measured due to recrystallization. At heating rates above 100 K/min, the most stable crystallites do not recrystallize during the DSC measure-

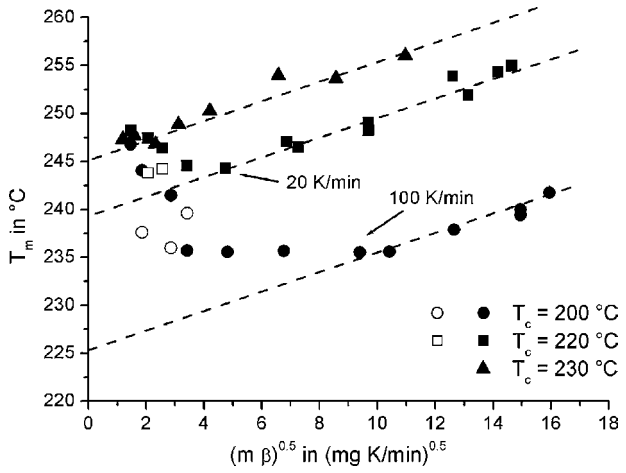

Fig. 8. Illers plot of the peak maximum temperatures of differently crystallized PET samples. The filled symbols represent the peak maximum temperature and the open symbols indicate the peak shoulders.

ment. The results at higher heating rates allow extrapolation to T_{m0}. The extrapolation of the lines in Fig. 8 can be taken as a good estimation for the melting temperatures of the crystallites grown at T_c. The values are listed in Table 1.

The use of fast heating rates together with the Illers plot allows the temperature of fusion of metastable crystallites to be determined. The relative fast and accurate determination of T_{m0} also allows rapid determination of the equilibrium melting temperature.

Minakov et al. [6] studied the melting and reorganization behavior of PET in a much broader range of heating rates (2–162,000 K/min) using different sample masses between 16 mg and 0.6 μg and different instruments. In this paper also double peaks are shown at low heating rates which combine to one single peak at higher rates. However, the heating rate dependence of the main melting peaks is different to our results. A direct comparison of the data in Ref. [6] and our results is unfortunately not possible because of differences in the material. The PET used in Ref. [6] melts at about 15 K higher temperatures. This indicates different kinetics and structure. Furthermore, it is seems that samples were many times repeatedly crystallized above 200 °C. During storage in at this temperature chemical reactions like degradation, chain extension [23] or transesterification [24,25] can occur. Consequently, the crystallization kinetics and the subsequent melting behavior changes after several crystallization cycles. This was shown in our initial experiments. Another effect which may influence the crystallization, reorganization and melting is given by the large relative surface of the very small samples used in Ref. [6].

Table 1
Crystallization temperature T_c and estimated melting temperature T_{m0}

T_c (°C)	T_{m0} (°C)
200	225.4
220	239.4
230	245.0

4. Conclusions

The agreement between the measured results and the theoretical approaches shows that curves measured by the DSC822^e at fast heating rates can be analyzed both qualitatively and quantitatively. In order to do this, the standard calibration procedure is expanded to include faster heating rates and is employed for an overall calibration of the experimental setup. Commercially available crucibles and the sample robot are especially useful for sequential measurements at slow and fast heating rates.

The example of amorphous and semicrystalline PET shows that DSC analysis at fast heating rates is a useful tool for the investigation of metastable structures in polymers. At fast heating rates, the reorientation processes is partially suppressed. This allows the original structure to be analyzed. The original degree of crystallinity can be measured directly and the crystallite size estimated. In the case of metastable semicrystalline PET, the melting temperature of the original crystallites can be determined using fast heating rates and the Illers rule.

Depending on the structure of the material, the exponential equation (3) and the Illers plot can be used to determine the minimum heating rate at which practically no reorientation occurs in the relative stable crystallites of the sample. Furthermore, it is shown that the heating rate dependence of the glass transition temperature of rapidly cooled material is caused by smearing due to heat transfer.

In practice, the increase achieved in DSC sample throughput is also important. This is supported by a simple and universal calibration procedure (FlexCal^{TM}). This allows slow and fast measurements to be performed with the same set of calibration parameters and permits the use of the sample robot together with automatic evaluation procedures.

Acknowledgement

The author would like to thank P. Callens (Agfa Gevaert N.V., Belgium) for helpful discussions and for supplying samples.

Appendix A

The enthalpic glass transition temperature is heating rate invariant. This is a direct consequence of the law of energy conservation. We will show this here because it was a point of discussion with a reviewer of the manuscript and seems not clear in general.

If a supercooled liquid is cooled from a temperature T_1 above the glass transition to T_2 below the glass transition, the enthalpy decreases from H_1 to H_2 by $\Delta H = H_1 - H_2$. If no structural relaxation occurs at T_2 before the sample is reheated to T_1 the enthalpy changes by $-\Delta H$ and the enthalpy differences between the cooling and subsequent heating cycle is zero. This means:

$$\int_{T_2}^{T_1} C_{p-}(T)\mathrm{d}T = \int_{T_2}^{T_1} C_{p+}(T)\mathrm{d}T = \Delta H \tag{A1}$$

where C_{p-} is the heat capacity measured during cooling and C_{p+} is the heat capacity from the subsequent heating run.

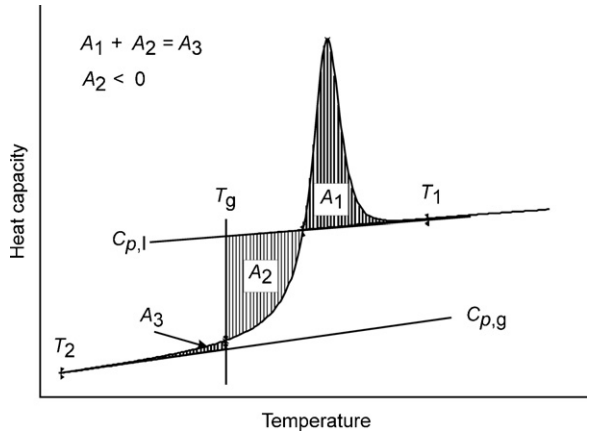

Fig. A1. Schema of the evaluation of the enthalpic glass transition temperature.

According to Ref. [11] the enthalpic glass transition temperature can be determine by a graphical method shown in Fig. A1. It is obvious, that this method is equivalent to Eq. (A2) for the heating case:

$$\int_{T_2}^{T_g}(C_{p+}(T)-C_{p,g}(T))\mathrm{d}T=-\int_{T_g}^{T_1}(C_{p+}(T)-C_{p,l}(T))\mathrm{d}T \tag{A2}$$

where $C_{p,g}$ and $C_{p,l}$ are the heat capacities of the glass and of the liquid, respectively. These functions are determined from the measured heat capacity curve (or heat flow curve) around T_1 or T_2 by linear approximation and extrapolation into the glass transition range. By algebraic rearrangment of Eq. (A2) follows:

$$\int_{T_2}^{T_g}C_{p+}(T)\mathrm{d}T+\int_{T_g}^{T_1}C_{p+}(T)\mathrm{d}T=\int_{T_2}^{T_1}C_{p+}(T)\mathrm{d}T$$
$$=\int_{T_g}^{T_1}C_{p,l}(T)\mathrm{d}T+\int_{T_2}^{T_g}C_{p,g}(T)\mathrm{d}T \tag{A3}$$

If we assume that T_g' is the enthalpic glass transition temperature at cooling, it follows in analogy to Eq. (A3):

$$\int_{T_2}^{T_1}C_{p-}(T)\mathrm{d}T=\int_{T_g'}^{T_1}C_{p,l}(T)\mathrm{d}T+\int_{T_2}^{T_g'}C_{p,g}(T)\mathrm{d}T \tag{A4}$$

The left sides of Eqs. (A3) and (A4) are equivalent due to Eq. (A1). Consequently, Eq. (A5) is valid:

$$\int_{T_g}^{T_1}C_{p,l}(T)\mathrm{d}T+\int_{T_2}^{T_g}C_{p,g}(T)\mathrm{d}T$$
$$=\int_{T_g'}^{T_1}C_{p,l}(T)\mathrm{d}T+\int_{T_2}^{T_g'}C_{p,g}(T)\mathrm{d}T \tag{A5}$$

The heat capacity outside of the transition region is independent on the measurement conditions. Thus the functions $C_{p,g}(T)$ and $C_{p,l}(T)$ are on the left and right side of Eq. (A5) identical. Eq. (A5) is valid if $T_g'=T_g$. Consequently the enthalpic glass transition temperature measured by heating is always identical to the enthalpy glass transition temperature at the previous cooling process. The prerequisite of this result is, that the structural relaxation in the glassy state between the cooling and the heating process can be neglected. This is fulfilled then the T_2 is sufficiency below the glass transition region.

Appendix B

In this paragraph we derive an approximation equation for the heating rate dependence of the apparent glass transition temperature. It is assumed that the material was cooled at a rate β_c so that for all the experiments discussed the cooling rate is faster than the heating rate and possible exothermal and endothermal overshoots can be neglected. The shape of the DSC curve in the glass transition region is then given by a step-like increase in the heat flow without a relaxation peak. Furthermore, the heating rate should not be too slow in order to prevent large appreciable structural relaxation in the glassy state during heating. The resulting "exothermal overshot" should small enough that it is practically not affected by smearing. Sharp and high endothermal overheating peaks may be occurring if the heating rate is in the order of the cooling rate or higher. In the interesting heating rate region ($\beta<-\beta_c$) the endothermal overheating peaks are small and have a marginal influence. Thus, the heating rate dependence of the glass transition temperature is mainly determined by the smearing of the DSC curves due to heat transfer between sample and sensor.

The influence of the heat transfer path on the measured signal can be described by a Green's function $G(t)$ [13]. This function describes the dynamic behavior of a system and can be measured for example as the response to a sharp impulse, e.g. crystallization of a supercooled pure melt. The relation between the measured signal, $\Phi_m(t)$, and the heat flow into the sample, $\Phi(t)$, is given by a convolution product:

$$\Phi_m(t)=\int_0^t G(t-t')\Phi(t')\mathrm{d}t' \tag{B1}$$

For simplification, we describe the step-like change in the heat capacity of the sample by a linear function:

$$C(T)=\begin{cases}C_g, & \text{for } T<T_0\\ C_g+AT, & \text{for } T\le T\le T_0+\Delta T\\ C_g+\Delta C, & \text{for } T>T_0+\Delta T\end{cases} \tag{B2}$$

where C_g is the (constant) heat capacity in the glassy state, ΔC the heat capacity step-height at the glass transition, T_0 the onset temperature of the glass transition, and ΔT is the width. The slope A is $A=\Delta C/\Delta T$. The glass transition temperature, T_g, is defined as the temperature at the half step-height:

$$C(T_g)=C_g+\frac{\Delta C}{2} \tag{B3}$$

The simplest model for the heat transfer path is a connection of a thermal resister and a heat capacity. The Green's function of such a system is an exponential function:

$$G(t)=\tau^{-1}\exp\left(-\frac{t}{\tau}\right) \tag{B4}$$

where τ is the time constant.

The relation between temperature and time is given by the constant heating rate β:

$$T(t) = T_s + \beta t \tag{B5}$$

where T_s is the start temperature.

The heat flow is

$$\Phi = C\beta \tag{B6}$$

If the experiment starts at a sufficiently low temperature ($T_0 - T_s \gg \beta\tau$), the start-up effects disappears at T_0 and for temperatures below T_0, Eq. (B1) yields an unsmeared measured heat flow ($\Phi_m(T) = \Phi(T)$ for $T < T_0$). In the case that the heating rate is not too fast ($\Delta T \leq \beta\tau$), we can neglect the behavior of $C(T)$ for $T > T_0 + \Delta T$ because the half step-height in the measured Φ_m curve is between T_0 and $T_0 + \Delta T$. If we assume a width of the glass transition of $\Delta T = 20$ K and a time constant of $\tau = 2$ s, the maximum heating rate is in the order of 600 K/min. For the relevant heating rate and temperature range, the measured heat flow is given by introducing Eqs. (B2), (B4–B6) into (B1):

$$\Phi_m(T_0 \leq t \leq T_0 + \Delta T) = C_g\beta + \frac{A\beta^2}{\tau}\int_{t(T_0)}^{t(T\leq T_0+\Delta T)} (t' - t(T_0)) \exp\left(-\frac{t-t'}{\tau}\right) dt' \tag{B7}$$

If we set $t_0 = t(T_0)$, the solution of Eq. (B6) is

$$\Phi_m(t) = \beta\left[C_g + A\beta(t - t_0) - A\beta\tau\left(1 - \exp\left(-\frac{t-t_0}{\tau}\right)\right)\right] \tag{B8}$$

We define t_{g0} as the time at which the sample reaches the glass transition temperature. The time t_g at which the glass transition temperature is measured is larger than t_{g0}, but the heat flow is the same:

$$\Phi(t_{g0}) = \Phi_m(t_g) \tag{B9}$$

With

$$\Phi(t_{g0}) = \beta(C_g + A\beta(t_{g0} - t_0)) \tag{B10}$$

it follow from Eqs. (B8) to (B10) that

$$t_g = t_{g0} + \tau\left(1 - \exp\left(-\frac{t_g - t_0}{\tau}\right)\right) \tag{B11}$$

To obtain the related temperatures, the times have to be substituted using Eq. (B5): $t_g = (T_g - T_s)/\beta$, $t_{g0} = (T_{g0} - T_s)/\beta$, and$t_0$=$(T_0 - T_s)/\beta$. From Eq. (B11) follows that

$$T_g = T_{g0} + \beta\tau\left(1 - \exp\left(-\frac{T_g - T_0}{\beta\tau}\right)\right) \tag{B12}$$

This transcendental equation has a solution, but for practical purposes it is not easily to handle. We therefore substitute T_g in the exponent with the linear approximation of Eq. (B12), $T_g = T_{g0} + \beta\tau$. For the heating rate dependence of the measured glass transition temperature it then follows that

$$T_g(\beta) = T_{g0} + \beta\tau\left(1 - \exp\left(-\frac{T_{g0} - T_0}{\beta\tau} - 1\right)\right) \tag{B13}$$

This equation is valid for heating rates with

$$\beta \leq \frac{2(T_{g0} - T_0)}{\tau} \tag{B14}$$

References

[1] C. Schick, E. Donth, Phys. Scr. 43 (1991) 423.
[2] B. Wunderlich, Macromolecular Physics, vol. 1, Academic Press, New York, 1973;
B. Wunderlich, Macromolecular Physics, vol. 3, Academic Press, New York, 1980.
[3] H.G. Zachmann, Fortschr. Hochpolym. Forsch. 3 (1964) 581.
[4] T.F.J. Pijpers, V.B.F. Mathot, B. Goderis, R.L. Scherrenberger, E.W. van der Vegte, Macromolecules 33 (2002) 3601.
[5] V.B.F. Mathot, B. Goderis, H. Reynaers, Fibers Text. East. Eur. 11 (2003) 20.
[6] A.A. Minakov, D.A. Mordvintsev, C. Schick, Polymer 45 (2004) 3755.
[7] A.A. Minakov, D.A. Mordvintesv, R. Tol, C. Schick, Thermochim. Acta 442 (2006) 25.
[8] G.W.H. Höhne, H.K. Camenga, W. Eysel, E. Gmelin, W. Hemminger, Thermochim. Acta 160 (1990) 1.
[9] M.J. Richardson, in: V.B.F. Mathot (Ed.), Calorimetry and Thermal Analysis of Polymers, Hanser Publishers, Munich, 1994, p. 170ff.
[10] M.J. Richardson, N.G. Savill, Polymer 16 (1975) 753.
[11] C.T. Moynihan, A.J. Easteal, M. DeBolt, J. Tucker, J. Am. Ceram. Soc. 59 (1976) 12.
[12] C.T. Moynihan, A.J. Easteal, J. Wilder, J. Chem. Phys. 78 (1974) 2673.
[13] J.E.K. Schawe, C. Schick, G.W.H. Höhne, Thermochim. Acta 244 (1994) 49.
[14] J.E.K. Schawe, J. Polym. Sci. B: Polym. Phys. 36 (1998) 2165.
[15] M.J. Richardson, in: G. Allen (Ed.), Comprehensive Polymer Science, vol. 1, Pergamon Press, Oxford, 1989, p. 867ff.
[16] M. Alsleben, C. Schick, W. Mischok, Thermochim. Acta 187 (1991) 261.
[17] V.B.F. Mathot, R.L. Scherrenberg, T.F.J. Pijpers, W. Bras, J. Thermal. Anal. 46 (1996) 681.
[18] D.J. Blundell, D.R. Beckett, P.H. Willcocks, Polymer 22 (1981) 704.
[19] A. Mehta, U. Gaur, B. Wunderlich, J. Polym. Sci. Polym. Phys. Ed. 16 (1978) 289.
[20] K.-H. Illers, Eur. Polym. J. 40 (1974) 911.
[21] G. Wang, I.R. Harrison, Thermochim. Acta 230 (1993) 309.
[22] G. Wang, I.R. Harrison, Thermochim. Acta 231 (1994) 203.
[23] M. Paci, F.P. La Mantia, Polym. Degrad. Stab. 61 (1998) 417.
[24] J. Kugler, J.W. Gilmer, D. Wiswe, H.-G. Zachmann, K. Hahn, E.W. Fischer, Macromolecules 20 (1987) 1116.
[25] L. Liangbin, H. Rui, Z. Ling, H. Shiming, Polymer 42 (2001) 2085.